



## 1        **1. Introduction**

2        Ionic liquids (ILs) have received increasing attention because of such unique properties  
3        as negligible vapor pressure, good solubility to many organic and inorganic chemicals,  
4        and a wide range of temperatures in the liquid state [1,2]. Because of these features, ILs  
5        appeared as environmentally friendly alternatives for conventional volatile solvents [3–5].  
6        However, to assess the potential use of ILs as “greener” alternatives, other properties  
7        such as their toxicity and thermal/chemical stability should be fully characterized [6].  
8        Another outstanding feature is that ILs can be synthesized in numerous anion-cation  
9        combinations, which gives them the tunability to meet the specific requirements of a given  
10       application [7–9]. Consequently, ILs are regarded as emergent materials in various  
11       technological fields such as absorption refrigeration systems [10,11], electrolyte and  
12       electrode materials for batteries [12], optical media in photonic devices [13,14], etc.

13       Hydroxyl functionalized ILs endow conventional ILs with useful polarity/solvation  
14       properties and have shown great potential in the reversible absorption of gases, including  
15       carbon dioxide (CO<sub>2</sub>) and ammonia (NH<sub>3</sub>) [11,15,16]. Also, hydroxyl ILs exhibit better  
16       solubility of inorganic salts and enhanced hydrophilicity and enzyme activity, which means  
17       they can be used in a huge variety of applications [17]. For example, 1-(2-hydroxyethyl)-  
18       3-methylimidazolium tetrafluoroborate ([EtOHmim][BF<sub>4</sub>]), as the target IL in the present  
19       study, has been used in the synthesis of silver nanoparticles [17]; as a catalyst in the  
20       production of liquid fuel from renewable sources [18]; and in the absorption of hydrogen  
21       sulfide (H<sub>2</sub>S), CO<sub>2</sub> [19], and NH<sub>3</sub> [11]. To further expand the applications of hydroxyl ILs,  
22       and in particular of [EtOHmim][BF<sub>4</sub>], more detailed knowledge of their thermophysical  
23       properties is required. More specifically, given the potential use of [EtOHmim][BF<sub>4</sub>] as a  
24       solvent, it is essential to understand the thermodynamic behavior of its binary mixtures  
25       with water. However, despite its importance, there is little experimental data on pure IL,  
26       and very few researchers have reported the thermophysical properties of its binary  
27       mixtures with water or other compounds.

28       In an early experimental work, Kim et al. [20] used the boiling point method to measure  
29       the vapor pressure of binary mixtures of water + [EtOHmim][BF<sub>4</sub>] in the temperature range  
30       between 304.8 K and 475.2 K, and with the IL mole fraction between 0.2 and 0.8. They

1 correlated the results with an Antoine-type equation with very good fitting quality.  
2 Subsequently, Shokouhi et al. [19] determined the solubility and diffusivity of H<sub>2</sub>S and  
3 CO<sub>2</sub> in [EtOHmim][BF<sub>4</sub>]. They found that H<sub>2</sub>S and CO<sub>2</sub> are more soluble in the  
4 conventional IL 1-ethyl-3-methylimidazolium tetrafluoroborate ([emim][BF<sub>4</sub>]) and  
5 attributed this to a lower molar free volume in [EtOHmim][BF<sub>4</sub>]. Finally, they concluded  
6 that [EtOHmim][BF<sub>4</sub>] can be used to separate these two gases from each other. Our  
7 research group at Universitat Rovira i Virgili has also measured some of the  
8 thermophysical properties of the IL [EtOHmim][BF<sub>4</sub>], such as density (in the temperature  
9 range 293.15 K-373.15 K), viscosity (293.15 K-373.15 K), thermal conductivity (293.15 K  
10 -313.15 K), and heat capacity (273.15 K -373.15 K) [21]. All these properties were  
11 correlated as a function of temperature, and the maximum relative deviation between  
12 experimental and calculated values does not exceed 1.16% in any case. Furthermore,  
13 the density and viscosity of binary mixtures NH<sub>3</sub> + [EtOHmim][BF<sub>4</sub>] were also determined.  
14 Cera-Manjarres et al. [11] reported the vapor pressure measurements of NH<sub>3</sub> + protic ILs  
15 (HOILs) mixtures as potential working fluids for absorption refrigeration systems. Of all  
16 the HOILs investigated, [EtOHmim][BF<sub>4</sub>] was selected as the most suitable absorbent for  
17 NH<sub>3</sub>. More recently, the authors [22] used an advanced optical technique to determine  
18 the mutual diffusion coefficients in binary mixtures of water + [EtOHmim][BF<sub>4</sub>] throughout  
19 the IL mass fraction range between 298.15 K and 313.15 K. We also tested the prediction  
20 ability of four thermodynamic models and analyzed the influence of using different excess  
21 Gibbs energy (g<sup>E</sup>) models to calculate the relevant thermodynamics. The present study  
22 is effort further attempt by the authors to characterize the thermodynamic behavior of  
23 binary mixtures of water + [EtOHmim][BF<sub>4</sub>].

24 All previous studies show the limited experimental information available on the  
25 thermophysical properties of [EtOHmim][BF<sub>4</sub>], and especially on its aqueous binary  
26 mixtures. Such basic properties as density and refractive index need to be determined  
27 and understood so that equipment for commercial applications that use aqueous IL  
28 mixtures can be designed, scaled up and sized [23]. Of all the thermophysical properties  
29 of aqueous mixtures of ILs, density is probably the most widely studied because of its  
30 importance and experimental accessibility [24]. Also, several volumetric properties can  
31 be obtained from density measurements. Volumetric properties of binary mixtures depend

1 on the size, shape, and chemical nature of the components, and structural effects arising  
2 from interstitial accommodation due to differences in molar volume and free volume  
3 between solution components [25]. These properties provide useful information about the  
4 structure and solute-solute, solvent-solvent and solute-solvent interactions in a binary  
5 mixture. In comparison with density, the refractive index of aqueous IL mixtures has  
6 received considerably less attention. The refractive index of ILs is related to properties  
7 like structuredness, polarity, and relative hydrogen bonding donating and accepting  
8 ability, which are useful for determining solubilities, partition constants, and reaction rates  
9 [26]. Most techniques for determining refractive indices are highly expeditious and  
10 accurate, and usually require very small amounts of sample [27]. The refractive index is  
11 a fundamental optical property of matter and correlates with the composition,  
12 temperature, pressure, and light source wavelength of a liquid mixture [28]. In this regard,  
13 the variation of the refractive index with temperature and concentration is the basis of  
14 several optical methods that study heat and mass transfer and determine diffusion  
15 coefficients in transparent media [29–31]. Furthermore, understanding the temperature,  
16 concentration and dispersion coefficients of the refractive index is essential for real-time  
17 monitoring of processes of industrial and scientific interest.

18 The refractive index of liquid mixtures can be estimated from the refractive indices of the  
19 pure components and the density data of the mixture using mixing rule equations.  
20 Correlations such as Lorentz-Lorenz, Gladstone-Dale or Newton have been extensively  
21 tested and validated in the literature [24,28,31]. However, despite the close relationship  
22 between the two properties, few studies address the determination of density and  
23 refractive index in aqueous mixtures of ILs [4,23,24,27,32,33]. And most of the ones that  
24 do provide experimental data of the density and refractive index at only one temperature.  
25 Refractive index values are reported in the literature at a single wavelength, most  
26 commonly the yellow sodium D-line (wavelength,  $\lambda$ , 589.2 nm). Nevertheless, the  
27 potential application of ILs, for instance in variable focus lenses, requires an accurate  
28 characterization of the refractive index dispersion to ensure optimal performance [13].  
29 Furthermore, once the density and refractive index of a pure compound or a mixture are  
30 known, such related properties as electronic polarizability or molar refraction can be  
31 estimated. Therefore, a joint analysis of density and refractive index can provide highly

1 valuable information about the volumetric and optical behavior of pure ILs and aqueous  
2 IL mixtures.

3 The main aim of this study was to experimentally determine the density and refractive  
4 index of the binary mixture water + [EtOHmim][BF<sub>4</sub>] throughout the ionic liquid mass  
5 fraction range at several temperatures between 293.15 K and 323.15 K. All refractive  
6 index measurements were performed at five wavelengths in the visible-near infrared  
7 spectral range, from 589.2 nm to 935 nm. From the experimental data of density, the  
8 excess molar volume and the thermal expansion coefficient were obtained in the  
9 temperature range studied. Similarly, the refractive index data was used to obtain the  
10 coefficients of concentration, temperature and chromatic dispersion, and the deviation in  
11 the refractive index. Finally, a total of eleven refractive index mixing rules were  
12 quantitatively compared in terms of their performance for the studied mixture. To the best  
13 of our knowledge, this is the first time that wavelength-dependent refractive index data  
14 have been reported for binary aqueous IL mixtures. This study provides a wide variety of  
15 new experimental data, such as the concentration, temperature, and chromatic dispersion  
16 coefficients of the refractive index of an aqueous mixture of IL.

## 17 **2. Experimental section**

18 **Table 1** shows the specifications of the chemical used in the present study. Extra pure  
19 deionized water supplied by Acros Organics was used without further purification. Ionic  
20 liquid 1-(2-hydroxyethyl)-3-methylimidazolium tetrafluoroborate ([EtOHmim][BF<sub>4</sub>], initial  
21 mass fraction purity: >98%, CAS Number: 374564-83-7, Molecular Weight: 213.97 g/mol)  
22 was supplied by lolitec. To remove traces of water from [EtOHmim][BF<sub>4</sub>], it was kept under  
23 vacuum (0.03 mbar) with heating and stirring at 333.15 K for at least 48 h. The water  
24 content (<150 ppm) was determined using a Karl Fisher coulometer (Mettler Toledo,  
25 model C20). Mixtures of water + [EtOHmim][BF<sub>4</sub>] were prepared gravimetrically using an  
26 electronic balance manufactured by Sartorius with a resolution of 10<sup>-2</sup> mg/30 g. A total of  
27 11 samples (including pure components) were prepared at 0.1 intervals throughout the  
28 ionic liquid mass fraction. The estimated uncertainty in the mass fraction is in the range  
29 of ±0.0008 to ±0.0029. All the measurements were conducted in a small room with well  
30 controlled air temperature at atmospheric pressure.

1

Table 1. Specifications of chemical used in the present study.

Chemical name	CAS	Purity <sup>1</sup> (mass-fraction, %)	Purification Method	Water content	Supplier
[EtOHmim][BF <sub>4</sub> ] <sup>2</sup>	374564-83-7	>98	Vacuum desiccation	<150 ppm (Karl-Fischer)	Iolitec
Water	7732-18-5	99.998	-	-	Acros Organics

2

<sup>1</sup> Provided by the supplier.

<sup>2</sup> [EtOHmim][BF<sub>4</sub>] = 1-(2-hydroxyethyl)-3-methylimidazolium tetrafluoroborate.

3 Density measurements were made with an oscillating U-tube Anton Paar densitometer  
 4 (DMA 5000M) at temperatures ranging from 293.15 K to 323.15 K. The temperature  
 5 uncertainty was estimated to be  $\pm 0.01$  K. The expanded uncertainty (with 0.95 level of  
 6 confidence ( $k=2$ )) in density is in the range of  $\pm 0.0010$  to  $\pm 0.0056$  g·cm<sup>-3</sup>. The quantity of  
 7 sample required to fill the U-tube was about  $5 \times 10^{-3}$  L and was introduced into the  
 8 equipment with a syringe. Care was taken to prevent bubbles from appearing in the tube.  
 9 Before the beginning of the experiments, the densitometer was verified by measuring the  
 10 density of Millipore quality water and dry air according to the supplier's instructions and  
 11 the deviations were found to be within  $\pm 1 \times 10^{-5}$  g cm<sup>-3</sup>. The density measurements for  
 12 the binary mixture samples were made in triplicate and the average values were reported.  
 13 The maximum deviation never exceeded the uncertainty of our measurements.

14 The refractive indices were measured with an Abbe refractometer, model 60/LR,  
 15 manufactured by Bellingham and Stanley, with a resolution of  $5 \times 10^{-5}$ . Five light emitting  
 16 diodes, with wavelengths of 589.2 nm, 632.8 nm, 670 nm, 780 nm, and 935 nm, and  
 17 bandwidth around 20 nm, mounted on a home-built wheel were used as a light source.  
 18 The light beams were alternately directed into the refractometer through the optical  
 19 window. Since infrared light is invisible (and harmful) to the human eye, the refractometer  
 20 was equipped with a high sensitivity camera. All the measurements were performed  
 21 between 293.15 K and 323.15 K. The temperature during the experiments was controlled  
 22 by a high precision circulating thermal bath (NESLAB RTE-300). The temperature of the  
 23 measurement prism of the refractometer was monitored using the built-in temperature  
 24 sensor with an uncertainty of  $\pm 0.1$  K. The expanded uncertainty (with 0.95 level of  
 25 confidence ( $k=2$ )) in the refractive index is in the range of  $\pm 0.0002$  to  $\pm 0.0058$ . The  
 26 quantity of sample required was about  $1 \times 10^{-3}$  L. Prior to the beginning of the  
 27 experiments, the refractometer was calibrated by measuring the refractive index of

1 deionized water at known temperature. Deviations did not exceed  $7 \times 10^{-5}$ . A minimum of  
2 three readings were taken for each sample and the average value was reported. The  
3 maximum deviation was always within the uncertainty range of our measurements.

4 All measurements were made immediately after sample preparation and the techniques  
5 used to measure both properties (density and refractive index) are highly expeditious.  
6 Under these conditions, we can assume that the composition of the analyzed samples has  
7 not changed significantly due to the hydrolysis of the  $\text{BF}_4^-$  anion during the measurement  
8 time [34,35].

### 9 **3. Results and discussion**

10 In this section, the experimental and calculated properties are presented, and the trends  
11 discussed.

#### 12 **3.1. Density and volumetric properties**

13 The experimental density results are listed in Table 2. As expected, density increases with  
14 the IL mass fraction and decreases with temperature. Density values range from  $0.9880$   
15  $\text{g cm}^{-3}$  for pure water at  $323.15 \text{ K}$  to  $1.3685 \text{ g cm}^{-3}$  for pure ionic liquid at  $293.15 \text{ K}$ . From  
16 experimental density data in Table 2, it is observed that the influence of temperature on  
17 density is greater as the IL mass fraction increases.

18 The relative uncertainty of the density measurements was found to be always less than  
19 0.2%. The low uncertainty values observed are possible evidence that the hydrolysis of  
20 the  $\text{BF}_4^-$  anion has not altered our measurements to a significant extent. Moreover, we  
21 identified that the most important contribution to uncertainty in our density measurements  
22 is due to the purity of the IL, which is generally overlooked in most studies in the literature  
23 [36].

24 In the literature, there are no density data available for the binary mixture  $\text{H}_2\text{O}(1) +$   
25  $[\text{EtOHmim}][\text{BF}_4](2)$ . However, some values reported for the pure compounds are used for  
26 purposes of comparison. Figure 1 shows the deviations between the experimental density  
27 values obtained and those reported in the literature for water [4,23,24,37,38] and for ionic  
28 liquid  $[\text{EtOHmim}][\text{BF}_4]$  [19,39–42]. Figure 1 a) shows the small deviations between the

1 density values obtained and those reported in the literature for water. In most of the  
 2 experimental points investigated, the deviations oscillate between -0.005% and 0.005%.

3 *Table 2. Experimental density,  $\rho$ , of  $H_2O + [EtOHmim][BF_4]$  mixtures as a function of the ionic*  
 4 *liquid mass fraction,  $\omega_2$ , at temperatures,  $T^1$ , ranging from 293.15 K to 323.15 K and at*  
 5 *pressure,  $P^2$ , 0.1 MPa.*

$\omega_2 \pm u(\omega_2)^3$ IL mass fraction	Density, $\rho$ / g cm <sup>-3</sup>							U( $\rho$ ) <sup>4</sup> /g cm <sup>-3</sup>
	T /K							
	293.15	298.15	303.15	308.15	313.15	318.15	323.15	
0.00000 $\pm$ 0.00002	0.9982	0.9971	0.9957	0.9940	0.9922	0.9902	0.9880	$\pm$ 0.0010
0.0997 $\pm$ 0.0010	1.0274	1.0258	1.0241	1.0221	1.0200	1.0177	1.0153	$\pm$ 0.0012
0.2000 $\pm$ 0.0019	1.0588	1.0569	1.0547	1.0524	1.0500	1.0475	1.0449	$\pm$ 0.0018
0.2989 $\pm$ 0.0024	1.0964	1.0940	1.0915	1.0889	1.0862	1.0834	1.0805	$\pm$ 0.0022
0.3950 $\pm$ 0.0028	1.1346	1.1319	1.1291	1.1262	1.1232	1.1202	1.1165	$\pm$ 0.0028
0.4996 $\pm$ 0.0029	1.1703	1.1673	1.1642	1.1610	1.1577	1.1544	1.1510	$\pm$ 0.0032
0.6045 $\pm$ 0.0028	1.2037	1.2004	1.1970	1.1937	1.1903	1.1869	1.1836	$\pm$ 0.0036
0.6995 $\pm$ 0.0025	1.2395	1.2360	1.2324	1.2288	1.2252	1.2215	1.2179	$\pm$ 0.0040
0.8010 $\pm$ 0.0015	1.2767	1.2725	1.2693	1.2655	1.2618	1.2585	1.2544	$\pm$ 0.0044
0.8988 $\pm$ 0.0011	1.3211	1.3162	1.3130	1.3091	1.3053	1.3020	1.2975	$\pm$ 0.0050
1.0000 $\pm$ 0.0008	1.3685	1.3633	1.3600	1.3559	1.3518	1.3485	1.3439	$\pm$ 0.0056

6 <sup>1</sup> Standard uncertainty  $u(T) = 0.01$  K.

<sup>2</sup> Standard uncertainty  $u(P) = 10$  kPa.

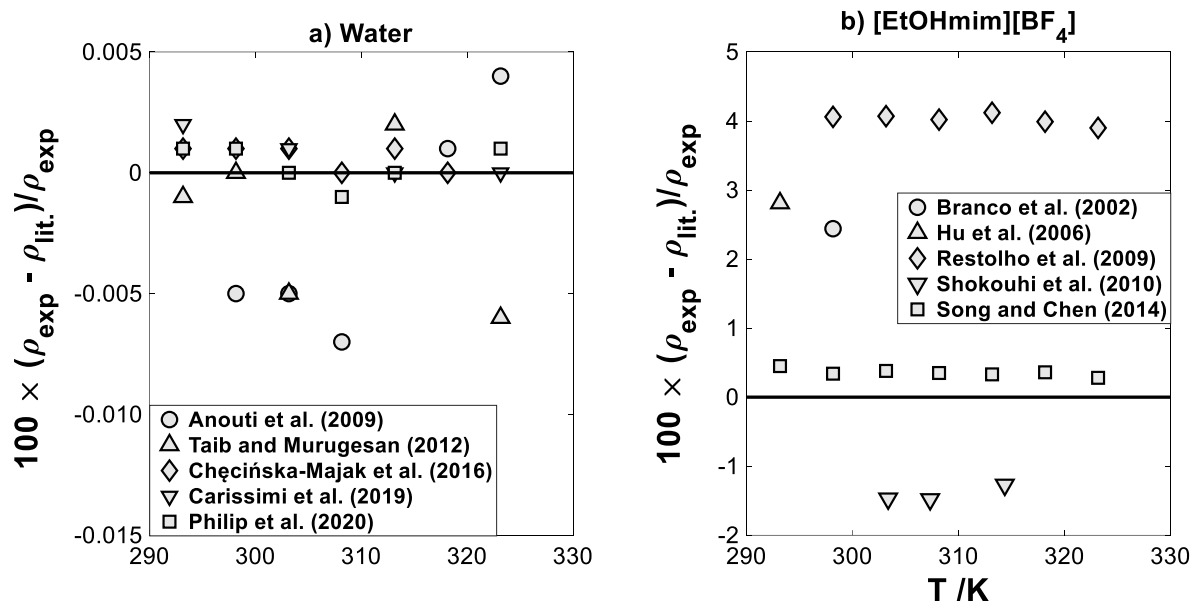
<sup>3</sup> Standard uncertainty  $u(\omega_2)$  is reported for each mass fraction studied.

<sup>4</sup> Expanded uncertainty with 0.95 level of confidence ( $k=2$ ).

7 However, relatively large deviations are generally observed for ionic liquid  
 8 [EtOHmim][BF<sub>4</sub>], as shown in Figure 1 b). These deviations can be attributed to different  
 9 purities of the ILs, handling of the samples, and measurement methods or experimental  
 10 procedures used. Furthermore, it can be observed that the deviations are positive, except  
 11 for the values reported by Shokouhi et al. [19] at temperatures slightly different from those  
 12 investigated in this study. Restolho et al. [41] and Song and Chen [42] reported density  
 13 values for [EtOHmim][BF<sub>4</sub>] at practically the same temperatures investigated in this study.  
 14 The deviations between our results and theirs are around 4% and 0.35%, respectively.  
 15 Therefore, there is excellent agreement between our values and Song and Chen's. Also,  
 16 an analysis of the values indicates that the values reported by Restolho et al. [41] are



1 somewhat smaller than the other density values reported in the literature for  
 2 [EtOHmim][BF<sub>4</sub>].



3  
 4 *Figure 1. Deviations between the experimental density values obtained in this study and those*  
 5 *from the literature for pure compounds at different temperatures: a) for water; and b) for ionic*  
 6 *liquid [EtOHmim][BF<sub>4</sub>].*

7 Furthermore, compared to [emim][BF<sub>4</sub>] [26], [EtOHmim][BF<sub>4</sub>] has higher density in the  
 8 temperature range. In this regard, the presence of the hydroxyl group in the cation of  
 9 [EtOHmim][BF<sub>4</sub>] gives rise to a stronger hydrogen bonding attraction, and causes cations  
 10 and anions to pack more tightly in [EtOHmim][BF<sub>4</sub>] than in [emim][BF<sub>4</sub>] [19].

11 The experimental density values were fitted using a second- and first-order polynomial  
 12 equation on IL mass fraction and temperature, respectively:

$$13 \quad \rho(\omega, T) / \text{g cm}^3 = \rho_{00} + \omega_2 * (\rho_{10} + \rho_{20} * \omega_2) + (T/K - T_0) * (\rho_{01} + \rho_{11} * \omega_2) \quad (1)$$

14 where  $T_0 = 293.15 \text{ K}$  and the coefficients  $\rho_{ij}$  are given in Table 3.

15 *Table 3. Coefficients of the fitting Equation (1) and goodness of fit ( $R^2$  and RMSE).*

Coefficients	$\rho_{00}$	$\rho_{01}$	$\rho_{10}$	$\rho_{11}$	$\rho_{20}$	$R^2$	RMSE
Value	9.989E-01	-3.802E-04	3.049E-01	-4.522E-04	6.082E-02	0.9992	3.3E-03

16

1 In Equation (1), the first term accounts for the density of pure water, the second for the  
 2 influence of the IL mass fraction on the mixture density, and the third term gives a sense  
 3 of the variation of the mixture density with temperature in the experimental range studied.

### 4 3.1.1. Excess molar volume

5 The excess molar volume of the H<sub>2</sub>O(1) + [EtOHmim][BF<sub>4</sub>](2) mixture was calculated from  
 6 the experimental data of density in Table 2 using Equation (2):

$$7 \quad V_m^E / \text{cm}^3 \text{mol}^{-1} = \frac{M_1 x_1 + M_2 x_2}{\rho} - \left( \frac{M_1 x_1}{\rho_1} + \frac{M_2 x_2}{\rho_2} \right) \quad (2)$$

8 The calculated excess molar volumes are tabulated in Table 1s in the supplementary  
 9 material. The excess molar volume is small, less than 1.4% of the molar volume of the  
 10 mixture. Furthermore, for the binary system studied, there is a considerable difference  
 11 between the molecular weights of water (18.0153 g/mol) and ionic liquid (213.97 g/mol).  
 12 In the molar representation, the measured points are concentrated at low mole fractions  
 13 and the commonly used fit with the Redlich-Kister polynomial does not work well.  
 14 Therefore, we used the following equation:

$$15 \quad V_m^E / \text{cm}^3 \text{mol}^{-1} = x_2 (1 - x_2) \frac{\sum_{i=0}^1 A_i (2x_2 - 1)^i}{1 + \sum_{i=1}^2 B_i (2x_2 - 1)^i} \quad (3)$$

16 which is considered more appropriate than the Redlich-Kister equation if the excess molar  
 17 volume is sharply asymmetrical [43]. In Equation (3), A<sub>i</sub> and B<sub>i</sub> are expressed as a linear  
 18 function on T:

$$19 \quad A_i = A_{i,0} + A_{i,1}(T/K - 273.15) \quad (4)$$

$$20 \quad B_i = B_{i,0} + B_{i,1}(T/K - 273.15) \quad (5)$$

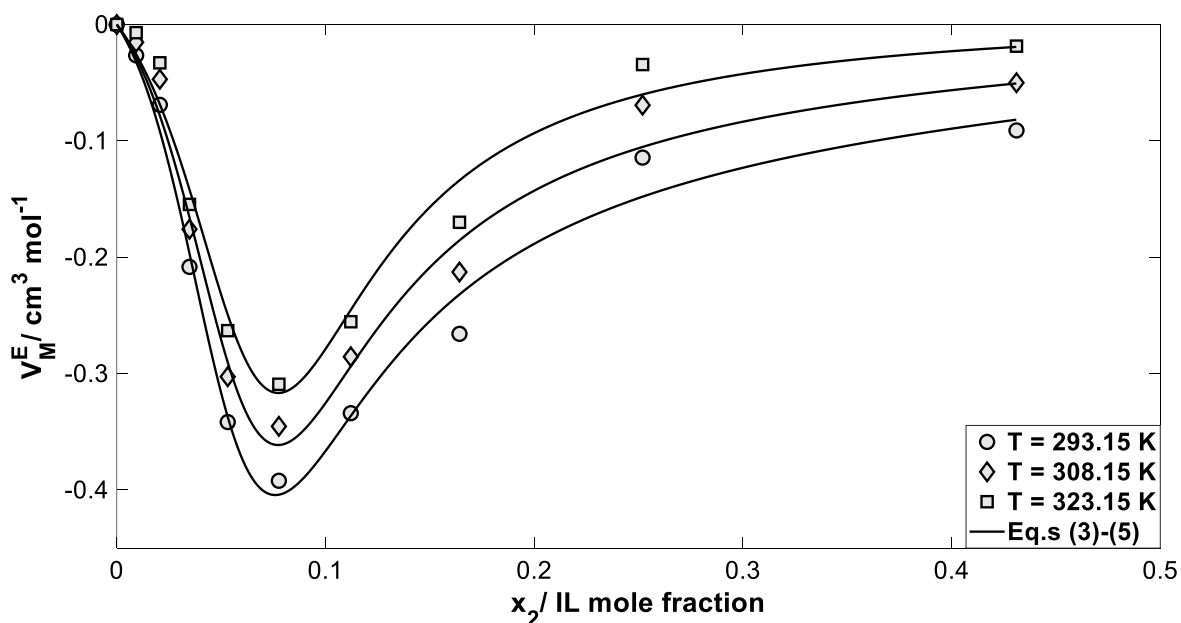
21 and the coefficients are given in Table 4.

22 *Table 4. Coefficients of the fitting Equation (3) and goodness of fit (R<sup>2</sup> and RMSE)*

Coefficients	A <sub>0,0</sub>	A <sub>0,1</sub>	A <sub>1,0</sub>	A <sub>1,1</sub>
Values	-4.126E-01	7.191E-03	-3.534E-01	7.543E-03
Coefficients	B <sub>1,0</sub>	B <sub>1,1</sub>	B <sub>2,0</sub>	B <sub>2,1</sub>
Values	2.146E+00	1.775E-03	1.164E+00	2.065E-03
R <sup>2</sup>	0.9763			
RMSE	0.021			

1 Therefore, we have simultaneously correlated the excess molar volume with temperature  
2 (T) and the IL mole fraction ( $x_2$ ) using Equations (3)-(5). The excess molar volume of the  
3 studied mixture and the fitting results using these equations are shown in Figure 2.

4 A glance at Figure 2 reveals that the excess molar volume is negative. Negative  $V_m^E$  values  
5 indicate that volume contracts in the mixture with respect to the ideal mixture. This  
6 contraction may be due to chemical interactions such as H-bond between the water  
7 molecules and the IL ions in the mixture. It may also be due to the geometrical fitting of  
8 one component into the other because of the different molar volumes of pure components  
9 [25].  $V_m^E$  reaches a minimum value ( $V_m^E \approx -0.4 \text{ cm}^3 \text{ mol}^{-1}$ ) at  $x_2 \approx 0.08$ . For  $x_2 \geq 0.08$ , the  
10 magnitude of  $V_m^E$  gets smaller as the concentration of water decreases in the mixture. This  
11 is probably due to the increased intermolecular interaction between the anionic and  
12 cationic species of [EtOHmim][BF<sub>4</sub>], which is favored over the interaction between water  
13 molecules and IL ions [24,25].



14

15 Figure 2. Excess molar volume as a function of the IL mole fraction at 298.15 K, 308.15 K, and  
16 323.15 K.

17 It is also observed that the magnitude of  $V_m^E$  decreases with temperature from 293.15 K to  
18 323.15 K at a given IL mole fraction. This is a common feature of several mixtures of  
19 imidazolium-based ILs with water [25]. It may be a consequence of the breaking of specific  
20 interactions in the IL-water mixture (usually H-bonds) when the temperature increases [24].

### 3.1.2. Thermal expansion coefficient

The isobaric thermal expansion coefficient,  $\beta$ , indicates changes in the volume of the mixture with temperature:

$$\beta/K^{-1} = -\frac{1}{\rho} \left( \frac{\partial \rho}{\partial T} \right)_p \quad (6)$$

The thermal expansion coefficient was obtained from the partial derivative of Equation (1) with respect to temperature, and its values are listed in Table 2s in the supplementary material. This table shows that  $\beta$  increases with IL mass fraction and temperature. There are no  $\beta$  data available for the mixture of interest, but we did find  $\beta$  data for the pure IL [EtOHmim][BF<sub>4</sub>]. Fakhraee et al.[17] investigated the thermodynamics and structural properties of several 1-(2-hydroxyethyl)-3-methyl imidazolium ionic liquids using molecular dynamics simulations and ab initio calculations. They reported values of  $\beta$  for [EtOHmim][BF<sub>4</sub>] at several temperatures. Here, for purposes of comparison we show our experimental values and their calculated values at two temperatures in Table 5. The relative deviation between experimental and calculated values is very small, -0.4% and 0.5% at 298.15 K and 313.15 K, respectively.

Table 5. Comparison between experimental and calculated thermal expansion coefficient,  $\beta \times 10^4 / K^{-1}$ , of [EtOHmim][BF<sub>4</sub>] at two temperatures, T, 298.15 K and 313.15 K.

T/ K	Thermal expansion coefficient, $\beta \times 10^4 / K^{-1}$		
	This study	Fakhraee et al. [17]	Deviation/ %
298.15	6.11 ± 0.05	6.13 ± 0.06	-0.4
313.15	6.16 ± 0.05	6.06 ± 0.06	0.5

We also calculated the excess thermal expansion coefficient,  $\beta^E$ :

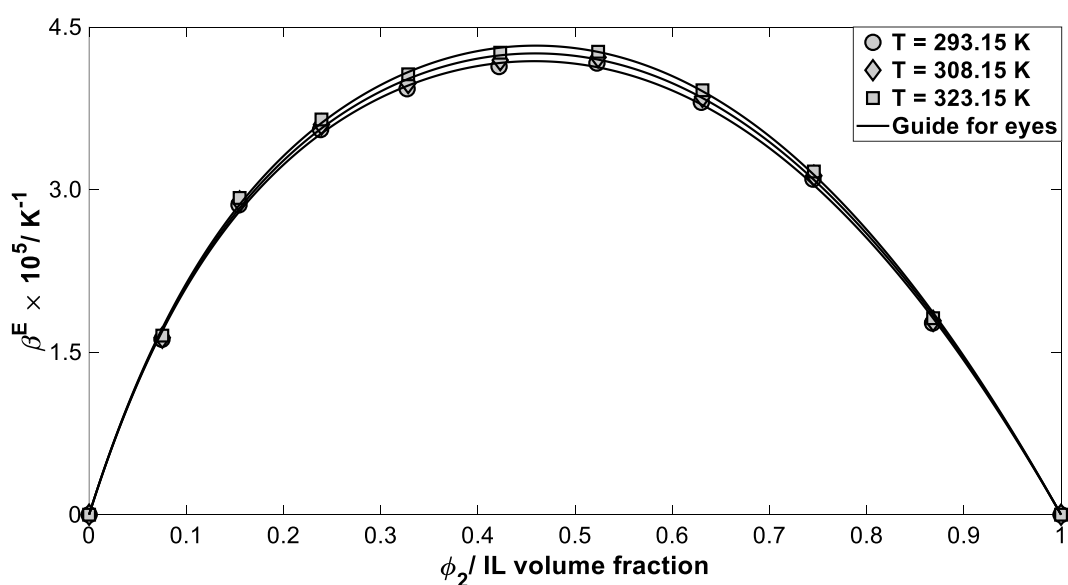
$$\beta^E / K^{-1} = \beta - \sum_{i=1}^2 \phi_i \beta_i^0 \quad (7)$$

where  $\beta_i^0$  is the thermal expansion coefficient of the pure components and  $\phi_i$  is the volume fraction of component i, defined by Equation (8):

$$\phi_i = \frac{x_i V_i}{\sum_{i=1}^2 x_i V_i} \quad (8)$$

Here,  $V_i$  is the molar volume of component i.

1 The values of  $\beta^E$  are given in Table 2s in the supplementary material. Figure 3 shows the  
 2 calculated excess thermal expansion coefficient for the mixture at three experimental  
 3 temperatures. It can be observed that this magnitude exhibits a positive deviation  
 4 throughout the IL volume fraction. From this figure, it is also obvious that it depends  
 5 heavily on the IL volume fraction.  $\beta^E$  increases with the IL volume fraction in the IL-dilute  
 6 region, reaches a maximum value ( $\beta^E \approx 4.3 \times 10^{-5} K^{-1}$ ) at  $\phi_2 \approx 0.45$ , and, from this point  
 7 onwards, decreases with the IL volume fraction. Figure 3 shows that the influence of  
 8 temperature on the excess thermal expansion coefficient is almost negligible.



9

10 Figure 3. Excess thermal expansion coefficient as a function of the IL volume fraction at 298.15  
 11 K, 308.15 K and 323.15 K.

### 12 3.2. Refractive index and related properties

13 Table 6 lists the measured refractive indices of the binary mixture  $H_2O + [EtOHmim][BF_4]$   
 14 at the temperatures and wavelengths studied. As expected, the refractive index increases  
 15 with the IL mass fraction, but decreases with temperature and wavelength.

16 No comparable refractive index data were found in the literature for the pure ionic liquid  
 17 and the binary mixture studied here. Thus, literature data on refractive index for pure  
 18 water at the studied temperatures and wavelengths are used for comparison.

1 Table 6. Experimental refractive index,  $n$ , of  $H_2O + [EtOHmim][BF_4]$  mixtures with ionic liquid  
 2 mass fractions,  $\omega_2$ , from 0 to 1, at temperatures,  $T^1$ , ranging from 293.2 K to 323.2 K, at  
 3 pressure,  $P^2$ , 0.1 MPa, and different wavelengths,  $\lambda$ .

$\omega_2 \pm u(\omega_2)^3/IL\ mass\ fraction$	Refractive index, $n$							$U(n)^4$
	T /K							
	293.2	298.2	303.2	308.2	313.2	318.2	323.2	
$\lambda = 589.2\ nm$								
0.00000 $\pm$ 0.00002	1.3334	1.3328	1.3323	1.3316	1.3309	1.3302	1.3293	0.0002
0.0997 $\pm$ 0.0010	1.3441	1.3423	1.3415	1.3409	1.3398	1.3391	1.3380	0.0006
0.2000 $\pm$ 0.0019	1.3527	1.3518	1.3509	1.3501	1.3493	1.3482	1.3473	0.0012
0.2989 $\pm$ 0.0024	1.3620	1.3604	1.3596	1.3590	1.3580	1.3573	1.3563	0.0016
0.3950 $\pm$ 0.0028	1.3715	1.3704	1.3692	1.3681	1.3673	1.3662	1.3651	0.0022
0.4996 $\pm$ 0.0029	1.3809	1.3787	1.3777	1.3769	1.3760	1.3746	1.3738	0.0028
0.6045 $\pm$ 0.0028	1.3892	1.3883	1.3872	1.3860	1.3849	1.3839	1.3828	0.0034
0.6995 $\pm$ 0.0025	1.3986	1.3974	1.3966	1.3956	1.3943	1.3934	1.3923	0.0040
0.8010 $\pm$ 0.0015	1.4081	1.4070	1.4061	1.4050	1.4041	1.4030	1.4020	0.0046
0.8988 $\pm$ 0.0011	1.4172	1.4161	1.4151	1.4138	1.4132	1.4122	1.4112	0.0050
1.0000 $\pm$ 0.0008	1.4267	1.4252	1.4243	1.4233	1.4221	1.4211	1.4198	0.0058
$\lambda = 632.8\ nm$								
0.00000 $\pm$ 0.00002	1.3323	1.3316	1.3311	1.3304	1.3297	1.3290	1.3282	0.0002
0.0997 $\pm$ 0.0010	1.3419	1.3411	1.3398	1.3390	1.3384	1.3374	1.3364	0.0006
0.2000 $\pm$ 0.0019	1.3510	1.3504	1.3492	1.3485	1.3474	1.3464	1.3456	0.0012
0.2989 $\pm$ 0.0024	1.3604	1.3596	1.3588	1.3580	1.3565	1.3552	1.3545	0.0016
0.3950 $\pm$ 0.0028	1.3702	1.3690	1.3681	1.3664	1.3658	1.3650	1.3636	0.0022
0.4996 $\pm$ 0.0029	1.3791	1.3775	1.3765	1.3751	1.3744	1.3731	1.3722	0.0028
0.6045 $\pm$ 0.0028	1.3881	1.3870	1.3857	1.3843	1.3833	1.3825	1.3816	0.0034
0.6995 $\pm$ 0.0025	1.3970	1.3959	1.3948	1.3939	1.3929	1.3914	1.3904	0.0040
0.8010 $\pm$ 0.0015	1.4063	1.4054	1.4044	1.4034	1.4024	1.4016	1.4003	0.0046
0.8988 $\pm$ 0.0011	1.4153	1.4142	1.4132	1.4123	1.4115	1.4106	1.4093	0.0050
1.0000 $\pm$ 0.0008	1.4248	1.4234	1.4224	1.4212	1.4204	1.4196	1.4184	0.0058
$\lambda = 670\ nm$								
0.00000 $\pm$ 0.00002	1.3312	1.3307	1.3301	1.3295	1.3288	1.3281	1.3272	0.0002
0.0997 $\pm$ 0.0010	1.3408	1.3397	1.3388	1.3377	1.3370	1.3365	1.3350	0.0006
0.2000 $\pm$ 0.0019	1.3498	1.3487	1.3479	1.3467	1.3460	1.3448	1.3439	0.0012
0.2989 $\pm$ 0.0024	1.3594	1.3581	1.3575	1.3563	1.3556	1.3542	1.3533	0.0016
0.3950 $\pm$ 0.0028	1.3681	1.3675	1.3668	1.3656	1.3642	1.3635	1.3625	0.0022
0.4996 $\pm$ 0.0029	1.3774	1.3762	1.3754	1.3738	1.3732	1.3719	1.3709	0.0028
0.6045 $\pm$ 0.0028	1.3866	1.3857	1.3848	1.3835	1.3824	1.3818	1.3803	0.0034
0.6995 $\pm$ 0.0025	1.3957	1.3944	1.3938	1.3927	1.3916	1.3902	1.3894	0.0040
0.8010 $\pm$ 0.0015	1.4053	1.4042	1.4034	1.4024	1.4013	1.4002	1.3991	0.0046
0.8988 $\pm$ 0.0011	1.4141	1.4132	1.4125	1.4111	1.4102	1.4093	1.4082	0.0050
1.0000 $\pm$ 0.0008	1.4235	1.4222	1.4213	1.4204	1.4193	1.4183	1.4174	0.0056
$\lambda = 780\ nm$								
0.00000 $\pm$ 0.00002	1.3290	1.3285	1.3279	1.3273	1.3266	1.3259	1.3251	0.0002
0.0997 $\pm$ 0.0010	1.3385	1.3370	1.3361	1.3353	1.3343	1.3334	1.3319	0.0006
0.2000 $\pm$ 0.0019	1.3471	1.3464	1.3457	1.3446	1.3436	1.3426	1.3417	0.0010
0.2989 $\pm$ 0.0024	1.3565	1.3557	1.3543	1.3534	1.3524	1.3518	1.3509	0.0016
0.3950 $\pm$ 0.0028	1.3661	1.3651	1.3637	1.3631	1.3620	1.3608	1.3597	0.0022
0.4996 $\pm$ 0.0029	1.3752	1.3734	1.3722	1.3713	1.3703	1.3694	1.3684	0.0028
0.6045 $\pm$ 0.0028	1.3843	1.3832	1.3822	1.3810	1.3801	1.3787	1.3775	0.0034
0.6995 $\pm$ 0.0025	1.3934	1.3920	1.3908	1.3903	1.3887	1.3881	1.3868	0.0040
0.8010 $\pm$ 0.0015	1.4022	1.4011	1.4002	1.3991	1.3985	1.3972	1.3961	0.0044
0.8988 $\pm$ 0.0011	1.4119	1.4109	1.4098	1.4084	1.4074	1.4067	1.4059	0.0050

	1.0000 ±0.0008	1.4210	1.4199	1.4192	1.4183	1.4171	1.4162	1.4148	0.0056
	<b>λ = 935 nm</b>								
	0.00000 ±0.00002	1.3267	1.3260	1.3254	1.3248	1.3241	1.3234	1.3226	0.0002
	0.0997 ±0.0010	1.3363	1.3351	1.3337	1.3328	1.3320	1.3311	1.3305	0.0006
	0.2000 ±0.0019	1.3448	1.3439	1.3429	1.3420	1.3408	1.3399	1.3390	0.0010
	0.2989 ±0.0024	1.3541	1.3530	1.3520	1.3513	1.3504	1.3494	1.3482	0.0016
	0.3950 ±0.0028	1.3632	1.3622	1.3617	1.3608	1.3597	1.3590	1.3579	0.0022
	0.4996 ±0.0029	1.3728	1.3717	1.3710	1.3696	1.3685	1.3673	1.3669	0.0028
	0.6045 ±0.0028	1.3814	1.3806	1.3794	1.3787	1.3777	1.3768	1.3760	0.0034
	0.6995 ±0.0025	1.3907	1.3895	1.3884	1.3876	1.3868	1.3859	1.3847	0.0038
	0.8010 ±0.0015	1.4001	1.3992	1.3985	1.3972	1.3962	1.3954	1.3941	0.0044
	0.8988 ±0.0011	1.4092	1.4079	1.4068	1.4058	1.4048	1.4040	1.4030	0.0050
1	1.0000 ±0.0008	1.4185	1.4170	1.4162	1.4151	1.4140	1.4132	1.4119	0.0056

<sup>1</sup> Standard uncertainty  $u(T) = 0.1$  K.

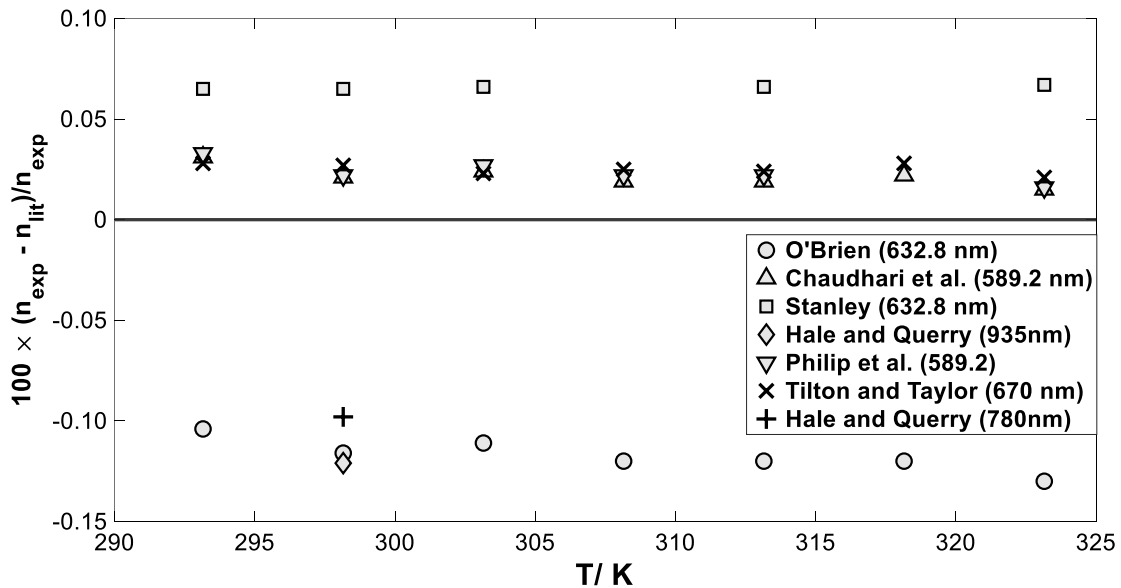
<sup>2</sup> Standard uncertainty  $u(P) = 10$  kPa.

<sup>3</sup> Standard uncertainty  $u(\omega_2)$  is reported for each mass fraction studied.

<sup>4</sup> Expanded uncertainty with 0.95 level of confidence ( $k=2$ ).

2

3 Figure 4 shows the deviations between the refractive index values obtained and those  
 4 reported in the literature for water [32,38,44–47]. As can be seen, the relative deviations  
 5 are generally very small and range between -0.12% and 0.07%.



6

7 Figure 4. Deviations between the experimental refractive index values obtained in this study and  
 8 those from the literature for pure water at different temperatures and wavelengths.

9 In the literature there are few values of the refractive index of water at 780 nm and 935  
 10 nm. We have been able to identify a single source from the literature at these

1 wavelengths (Hale and Querry [47] at 298 K). Therefore, this study also provides new  
 2 values for the refractive index of water at different temperatures for these wavelengths.

3 The refractive index of the pure [EtOHmim][BF<sub>4</sub>] is in the range from 1.4119 (at λ=935 nm  
 4 and T = 323.2 K) to 1.4267 (at λ=589.2 nm and T = 293.2 K), which is approximately 1.07  
 5 times higher than that of water under the same conditions. Moreover, compared to  
 6 [emim][BF<sub>4</sub>] [26], [EtOHmim][BF<sub>4</sub>] exhibits a higher refractive index because of the  
 7 hydroxyl group in the alkyl chain of its cation, which favors the formation of hydrogen  
 8 bonds with water.

9 Here, we have adopted a two-term Cauchy equation [9] to simultaneously investigate the  
 10 refractive index dependences on temperature, IL mass fraction and wavelength:

$$11 \quad n(T, \omega_2, \lambda) = A(T, \omega_2) + \frac{B(T, \omega_2)}{\lambda^2} \quad (9)$$

12 where  $A(T, \omega_2) = (a_{00} + a_{10} \cdot \omega_2 + a_{01} \cdot T + a_{11} \cdot \omega_2 \cdot T)$  and  $B(T, \omega_2) = (b_{00} + b_{10} \cdot \omega_2 + b_{01} \cdot$   
 13  $T + b_{11} \cdot \omega_2 \cdot T)$ . Using an eight-parameter fitting procedure, we determined the values of  
 14 the coefficients of Equation (9), which are listed in Table 7.

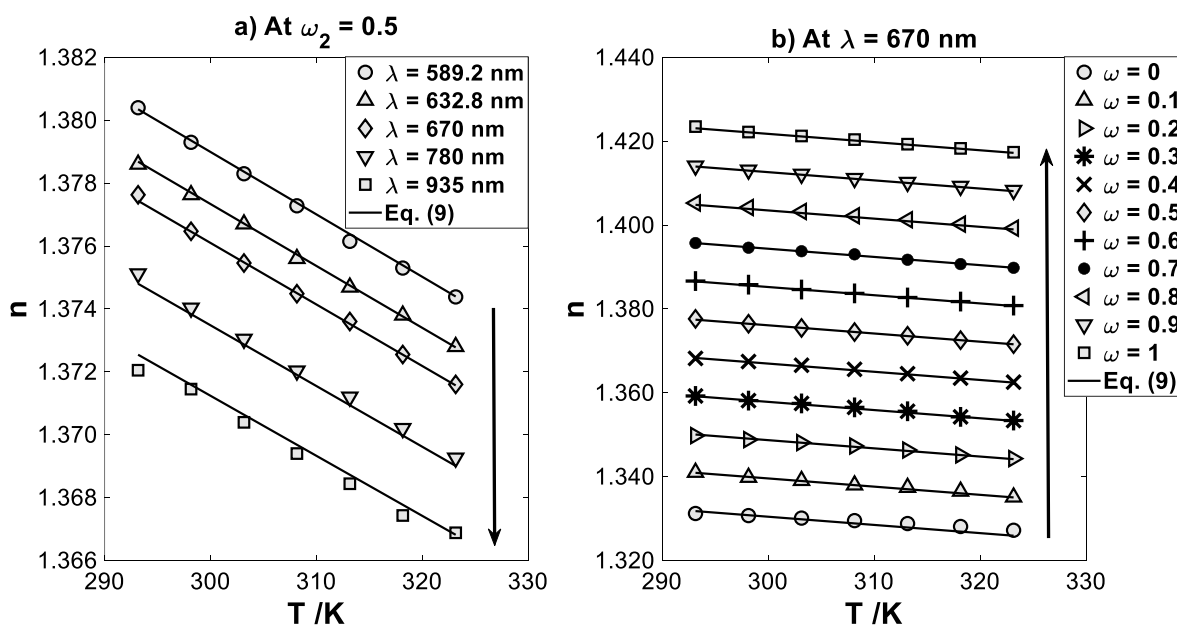
15 *Table 7. Coefficients of Equation (9) and goodness of fit (R<sup>2</sup> and RMSE)*

Coefficients	Value
$a_{00}$	1.3675
$a_{10}$	1.027E-02
$a_{01}$	-1.556E-04
$a_{11}$	-4.086E-05
$b_{00}$	5.859E-03
$b_{10}$	4.850E-04
$b_{01}$	-5.194E-06
$b_{11}$	-1.025E-07
R <sup>2</sup>	0.9999
RMSE	3.5E-04

16 The relative deviations between the experimental and calculated refractive indices values  
 17 do not exceed 0.1%. Equation (9) provides excellent estimates of the refractive index,  
 18 with a coefficient of determination R<sup>2</sup> = 0.9999 and root mean square error RMSE = 3.5E-  
 19 04.



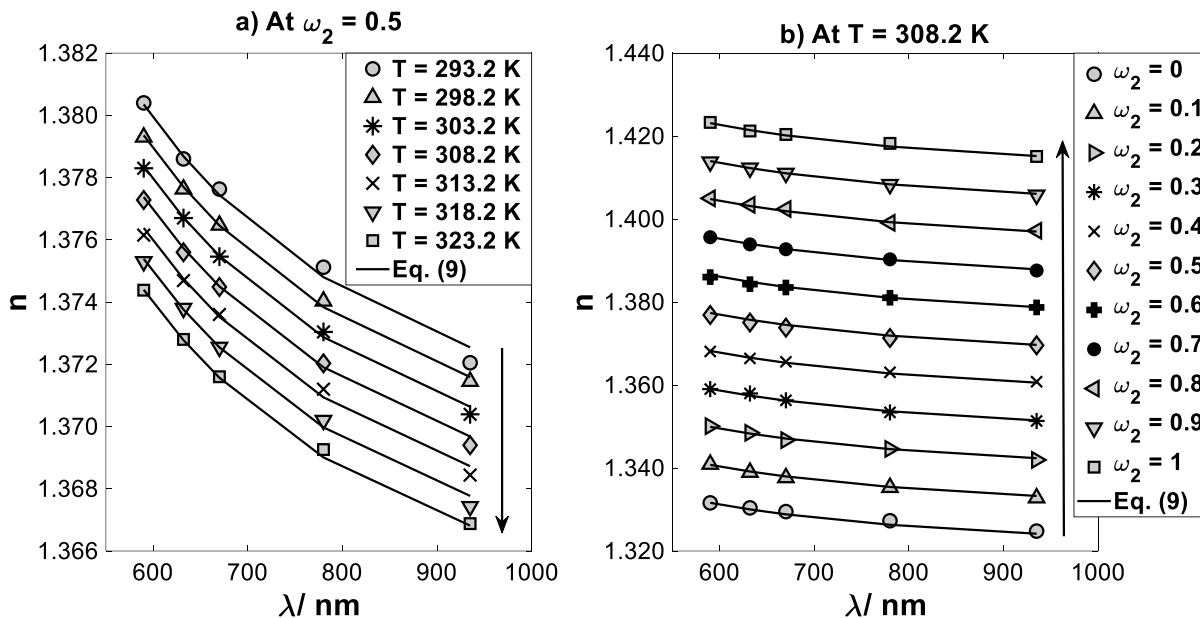
1 The analytical expression above enables us to obtain the dispersion relations of the  
 2 refractive index and interpolate refractive index values between measured points. As an  
 3 example, Figures 5 and 6 show the refractive index variations with temperature, IL mass  
 4 fraction and wavelength at selected experimental conditions. In these figures, the fitting  
 5 results of Equation (9) are also shown. As can be seen in Figure 5, the refractive index  
 6 decreases linearly with increasing temperature with a slope practically independent of  
 7 wavelength and IL mass fraction. Moreover, at a given IL mass fraction ( $\omega_2 = 0.5$ ), the  
 8 refractive index decreases with increasing wavelength. We also observed the refractive  
 9 index increases linearly with IL mass fraction at a given wavelength. A comparison  
 10 between Figure 5 a) and b) reveals that dependence of the refractive index on the IL mass  
 11 fraction is much stronger than on wavelength and temperature within the ranges of values  
 12 considered.



13  
 14 *Figure 5. Refractive index ( $n$ ) variation with temperature ( $T$ ) for the mixture  $H_2O +$   
 15  $[EtOHmim][BF_4]$ : a) At several wavelengths for  $\omega_2=0.5$ ; b) At several IL mass fractions for  $\lambda=670$   
 16 nm.*

17 In contrast with the linear relationship between the refractive index and the temperature  
 18 and IL mass fraction, we observed a nonlinear behavior of the refractive index with  
 19 variations in wavelength (see Figure 6). The refractive index for the studied mixture  
 20 presents normal dispersion, which means that as the wavelength increases the refractive

1 index decreases and the propagation velocity in the material increases [9]. A glance at  
 2 Figure 6 a) and b) shows that the dependence of the refractive index on the IL mass  
 3 fraction is much stronger than on the temperature within the ranges of values considered.



4  
 5 *Figure 6. Refractive index ( $n$ ) variation with wavelength ( $\lambda$ ) for the mixture  $H_2O +$*   
 6 *[EtOHmim][BF<sub>4</sub>]: a) At several temperatures for  $\omega_2=0.5$ ; b) At several IL mass fractions for*  
 7  *$T=308.2$  K.*

### 8 **3.2.1. Concentration, temperature, and dispersion derivatives of the refractive** 9 **index**

10 The concentration ( $\partial n/\partial \omega_2$ ), and temperature ( $\partial n/\partial T$ ) derivatives of the refractive index  
 11 (also known as optical contrast factors) can be directly obtained by analytical  
 12 differentiation of Equation (9). The calculated values of  $\partial n/\partial \omega_2$  and  $\partial n/\partial T$  are listed in  
 13 Tables 3s and 4s in the supplementary material, respectively. On one hand,  $\partial n/\partial \omega_2$   
 14 exhibits a positive sign, which indicates that the refractive index increases with the IL  
 15 mass fraction. On the other hand,  $\partial n/\partial T$  exhibits a negative sign, which indicates that  
 16 the refractive index decreases with temperature. Moreover, the absolute value of both  
 17 magnitudes shows a nonlinear decreasing behavior with the wavelength. Thus, the  
 18 influence of temperature and IL mass fraction on variation in the refractive index  
 19 decreases as the wavelength increases. Furthermore,  $\partial n/\partial T$  and  $\partial n/\partial \omega_2$  values are in

1 the same order as for conventional aqueous liquid mixtures,  $10^{-4} \text{ K}^{-1}$  and  $10^{-2}$ ,  
2 respectively.

3 The chromatic dispersion coefficient,  $\partial n/\partial \lambda$ , can also be calculated from Equation (9).  
4 The negative values at all the experimental temperatures and throughout the IL mass  
5 fraction range indicate that the refractive index always decreases with the wavelength.  
6 The values of  $\partial n/\partial \lambda$  are in the expected order of magnitude (i.e.,  $10^{-5} \text{ nm}^{-1}$ ), and are  
7 higher at shorter wavelengths. Thus, at shorter wavelengths, the dispersion is more  
8 intense, which is also representative of normal dispersion [9].

### 9 **3.2.2. Deviation in the refractive index**

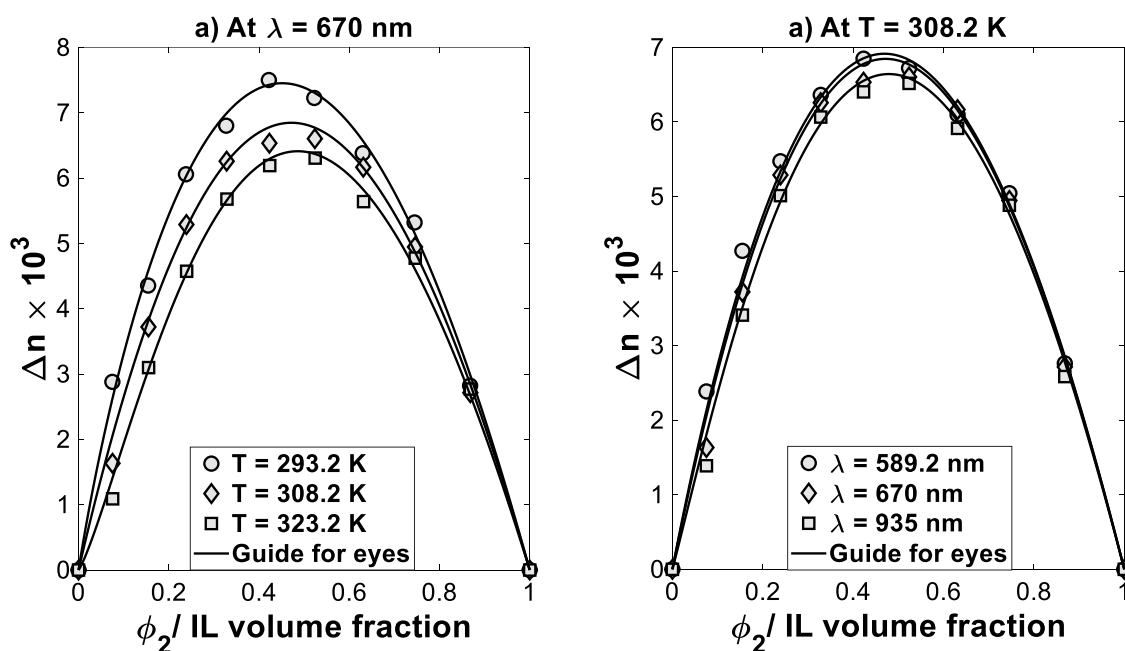
10 The deviation in the refractive index from ideal behavior  $\Delta n$  is defined as the difference  
11 between the refractive index of the mixture and the refractive index of the ideal mixture in  
12 the same thermodynamic state. As suggested by some authors [27,43,48], the refractive  
13 index for the ideal mixture is calculated in terms of volume fraction not mole fraction.  
14 Thus, the deviation in the refractive index was calculated using the following equation:

$$15 \quad \Delta n = n - \sum_{i=1}^2 n_i \phi_i \quad (10)$$

16 where  $n_i$  is the refractive index of the pure components, and  $\phi_i$  the volume fraction. The  
17 values of  $\Delta n$  are listed in Table 5s in the supplementary material.

18 Figure 7 shows the deviation in the refractive index of the mixture in different experimental  
19 conditions. As can be observed,  $\Delta n$  is positive throughout the IL volume fraction range  
20 and approaches a maximum of  $7.5 \times 10^{-3}$  at around  $\phi_2 \approx 0.42$ . In general, positive  
21 deviations in refractive index are considered to be associated with significant interactions  
22 in the mixtures [49]. Like Brocos et al. [48], we observed that the sign of the values of  $\Delta n$   
23 is opposite to the sign of the excess molar volumes ( $V_m^E$ ). Moreover, the extrema for both  
24 quantities,  $V_m^E$  and  $\Delta n$ , are found at the same IL mole fraction (note that  $\phi_2 \approx 0.42$   
25 corresponds to an IL mole fraction  $x_2 \approx 0.08$ ). This can be explained by the fact that  $\Delta n$   
26 is intrinsically related to  $V_m^E$  via the reduced free volume [27]. As stated by Anouti et al.  
27 [50], a negative  $V_m^E$  indicates that there is less free volume available than in an ideal  
28 solution, so photons will be more likely to interact with the ions or molecules in the mixture.  
29 Consequently, light will travel at a lower speed in the medium and its refractive index will

1 be higher than in an ideal solution. A comparison between Figure 2 and Figure 7 a) reveals  
 2 opposite trends for  $V_m^E$  and  $\Delta n$  with temperature. While the latter decreases, the former  
 3 increases with increasing temperature. Figure 7 b) shows that  $\Delta n$  also varies with the  
 4 wavelength, although the variation is quite small. As depicted,  $\Delta n$  slightly decreases with  
 5 increasing wavelength. A glance at Figure 7 a) and b) shows that the decrease in  $\Delta n$  with  
 6 temperature and wavelength is more pronounced at low and middle-range IL volume  
 7 fractions. Furthermore, our results also show that the dependence of  $\Delta n$  on wavelength  
 8 is much weaker than on temperature.



9

10 Figure 7. Deviation in refractive index,  $\Delta n$ , as a function of the IL volume fraction,  $\phi_2$ : a) At three  
 11 temperatures (298.2 K, 308.2 K, 323.2 K) for  $\lambda=670$  nm. b) At three wavelengths (589.2 nm, 670  
 12 nm, 935 nm) for  $T=308.2$  K.

13

### 3.2.3. Refractive index mixing rules

14 The refractive index of a liquid mixture can be estimated from the refractive indices of  
 15 pure components using mixing rule expressions. We used 11 mixing rules from the  
 16 literature to estimate the refractive index of the mixture water(1) + [EtOHmim][BF<sub>4</sub>](2).  
 17 Most of the expressions used are based upon the electromagnetic theory of light with the  
 18 implicit restriction that the molecules (or particles) may be regarded as dipoles or  
 19 assemblies of dipoles induced by an external field [51]. We made a quantitative

1 comparison of the refractive indices measured and the values predicted using the mixing  
2 rules selected. The average percentage deviation (APD) and maximal deviation  
3 (MaxDev) were used as the main criteria to evaluate the prediction ability of the mixing  
4 rules investigated.

5 The values of the APD and MaxDev for all the mixing rules studied are listed in [Table 6s](#)  
6 in the supplementary material. In general, the estimated values of the refractive index  
7 were found to be in good agreement with the experimental values. At all experimental  
8 temperatures and wavelengths, APD values do not exceed 0.3%, while MaxDev is about  
9 0.6 %. However, all mixing rules provide comparable results. Therefore, more advanced  
10 mixing rules do not lead to any improvement in comparison with the simple linear mixing  
11 rule (Arago-Biot). Moreover, deviations between experimental and calculated refractive  
12 index refractive values were larger at  $\phi_2 \approx 0.42$ , lower temperatures, and shorter  
13 wavelengths. As discussed above, in these experimental conditions, the non-ideality of  
14 the binary system studied is more pronounced.

15 The concentration contrast factor is an important parameter for several experimental  
16 techniques [29–31]. Thus, we also evaluated how the mixing rules calculated the  
17 concentration contrast factor of the mixture studied. The results are also listed in [Table 6s](#)  
18 in the supplementary material. In this case, the deviations were significantly higher than  
19 in the case of the refractive index calculations. The APD values were in the range from  
20 18.5% to 19.9%, while the MaxDev values were in the range from 18.9% to 20.3%. Again,  
21 a more advanced mixing rule leads to no essential improvement in comparison with the  
22 simple linear mixing rule (Arago-Biot).

#### 23 **4. Summary and conclusions**

24 The density and refractive index of binary mixtures of water + ionic liquid [EtOHmim][BF<sub>4</sub>]  
25 were measured throughout the ionic liquid mass fraction range, at atmospheric pressure  
26 and various temperatures between 293.15 K and 323.15 K. The refractive index was  
27 measured at five wavelengths between 589.2 nm and 935 nm.

28 Experimental density values range from 1.3439 g cm<sup>-3</sup> at 323.15 K to 1.3685 g cm<sup>-3</sup> at  
29 293.15 K for pure ionic liquid [EtOHmim][BF<sub>4</sub>]. Relatively large deviations are observed  
30 between the density values reported in different literature sources for this ionic liquid. The

1 influence of temperature on the density of the binary mixture studied is greater as the IL  
2 mass fraction increases. The excess molar volume ( $V_m^E$ ) is negative throughout the IL  
3 mole fraction range studied with a minimum of around  $V_m^E = -0.4 \text{ cm mol}^{-3}$  at an IL mole  
4 fraction of around 0.08.

5 The refractive index of the mixture increases with IL mass fraction but decreases with  
6 temperature and wavelength. The results of our investigation show that the refractive  
7 index of the mixture exhibit a linear dependence on IL mass fraction and temperature and  
8 a nonlinear dependence on wavelength. We successfully correlated the experimental  
9 refractive index with a two-term Cauchy equation in order to simultaneously investigate  
10 dependences on temperature, IL mass fraction and wavelength. The relative deviation  
11 between experimental and calculated refractive indices do not exceed 0.1%. The  
12 deviation in the refractive index was found to be positive throughout the composition  
13 range. The 11 mixing rules used to estimate the refractive index and concentration  
14 contrast factor of the binary mixture studied provide comparable results. Therefore, more  
15 advanced mixing rules do not lead to any essential improvement in comparison with the  
16 simple linear mixing rule (Arago-Biot).

## 17 **5. Supporting information**

18 The excess molar volumes, ( $V_m^E$ ), thermal expansion coefficient, ( $\beta$ ), and excess thermal  
19 expansion coefficient, ( $\beta^E$ ), are included in the supplementary material. Also included are  
20 the deviation in the refractive index as a function of the ionic liquid mass fraction,  
21 temperature and wavelength, and the performance indicators of the investigated  
22 refractive index mixing rules.

## 23 **6. Acknowledgments**

24 The authors from Universitat Rovira i Virgili acknowledge the financial support under  
25 Research project DPI2015-71306-R cofunded by the Ministry of Economy and  
26 Competitiveness of Spain and the European Regional Development Fund (FEDER). We  
27 also acknowledge the thoughtful comments on the paper of Prof. M. S. Larrechi and Dr.  
28 Daniel Salavera of the Universitat Rovira i Virgili. The authors from Université Libre de  
29 Bruxelles acknowledge financial support from the PRODEX program of the Belgian  
30 Federal Science Policy Office.

## 7. References

- [1] B. Mokhtarani, M.M. Mojtahedi, H.R. Mortaheb, M. Mafí, F. Yazdani, F. Sadeghian, Densities, refractive indices, and viscosities of the ionic liquids 1-methyl-3-octylimidazolium tetrafluoroborate and 1-methyl-3-butylimidazolium perchlorate and their binary mixtures with ethanol at several temperatures, *J. Chem. Eng. Data.* 53 (2008) 677–682. doi:10.1021/je700521t.
- [2] N. V. Sastry, N.M. Vaghela, P.M. Macwan, Densities, excess molar and partial molar volumes for water + 1-butyl- or, 1-hexyl- or, 1-octyl-3-methylimidazolium halide room temperature ionic liquids at  $T = (298.15 \text{ and } 308.15) \text{ K}$ , *J. Mol. Liq.* 180 (2013) 12–18. doi:10.1016/j.molliq.2012.12.018.
- [3] A. Kumar, T. Singh, R.L. Gardas, J.A.P. Coutinho, Non-ideal behaviour of a room temperature ionic liquid in an alkoxyethanol or poly ethers at  $T = (298.15 \text{ to } 318.15) \text{ K}$ , *J. Chem. Thermodyn.* 40 (2008) 32–39. doi:10.1016/j.jct.2007.06.002.
- [4] M. Anouti, M. Caillon-Caravanier, Y. Dridi, J. Jacquemin, C. Hardacre, D. Lemordant, Liquid densities, heat capacities, refractive index and excess quantities for {protic ionic liquids + water} binary system, *J. Chem. Thermodyn.* 41 (2009) 799–808. doi:10.1016/j.jct.2009.01.011.
- [5] S. Calixto, M. Rosete-Aguilar, F.J. Sanchez-Marin, O.L. Torres-Rocha, E.M. Martínez-Prado, M. Calixto-Solano, Optofluidic Compound Lenses Made with Ionic Liquids, in: S.T. Handy (Ed.), *Appl. Ion. Liq. Sci. Technol.*, InTech, Rijeka, 2011: pp. 495–516. doi:10.1007/978-3-662-44903-5.
- [6] M.G. Freire, C.M.S.S. Neves, I.M. Marrucho, J.A.P. Coutinho, A.M. Fernandes, Hydrolysis of tetrafluoroborate and hexafluorophosphate counter ions in imidazolium-based ionic liquids, *J. Phys. Chem. A.* 114 (2010) 3744–3749. doi:10.1021/jp903292n.
- [7] M. Tariq, P.A.S. Forte, M.F.C. Gomes, J.N.C. Lopes, L.P.N. Rebelo, Densities and refractive indices of imidazolium- and phosphonium-based ionic liquids: Effect of temperature, alkyl chain length, and anion, *J. Chem. Thermodyn.* 41 (2009) 790–798. doi:10.1016/j.jct.2009.01.012.
- [8] S. Govardhana Rao, T. Madhu Mohan, T. Vijaya Krishna, K. Narendra, B. Subba Rao, Thermophysical properties of 1-butyl-3-methylimidazolium tetrafluoroborate and N-methyl-2-pyrrolidinone as a function of temperature, *J. Mol. Liq.* 211 (2015) 1009–1017.

- 1       doi:10.1016/j.molliq.2015.08.019.
- 2   [9]   Y. Arosa, C.D. Rodríguez Fernández, E. López Lago, A. Amigo, L.M. Varela, O. Cabeza, R.  
3       de la Fuente, Refractive index measurement of imidazolium based ionic liquids in the Vis-  
4       NIR, *Opt. Mater. (Amst)*. 73 (2017) 647–657. doi:10.1016/j.optmat.2017.09.028.
- 5   [10]   M. Seiler, A. Kühn, F. Ziegler, X. Wang, Sustainable cooling strategies using new chemical  
6       system solutions, *Ind. Eng. Chem. Res.* 52 (2013) 16519–16546. doi:10.1021/ie401297u.
- 7   [11]   A. Cera-Manjarres, D. Salavera, A. Coronas, Vapour pressure measurements of  
8       ammonia/ionic liquids mixtures as suitable alternative working fluids for absorption  
9       refrigeration technology, *Fluid Phase Equilib.* 476 (2018) 48–60.  
10      doi:10.1016/j.fluid.2018.01.006.
- 11   [12]   M. Watanabe, M.L. Thomas, S. Zhang, K. Ueno, T. Yasuda, K. Dokko, Application of Ionic  
12      Liquids to Energy Storage and Conversion Materials and Devices, *Chem. Rev.* 117 (2017)  
13      7190–7239. doi:10.1021/acs.chemrev.6b00504.
- 14   [13]   J.A. Nóvoa-López, H. Michinel, E. López-Lago, *Ionic Liquids in Separation Technology*,  
15      Elsevier, 2014. doi:10.1016/C2013-0-00056-4.
- 16   [14]   C. Chiappe, P. Margari, A. Mezzetta, C.S. Pomelli, S. Koutsoumpos, M. Papamichael, P.  
17      Giannios, K. Moutzouris, Temperature effects on the viscosity and the wavelength-  
18      dependent refractive index of imidazolium-based ionic liquids with a phosphorus-containing  
19      anion, *Phys. Chem. Chem. Phys.* 19 (2017) 8201–8209. doi:10.1039/c6cp08910k.
- 20   [15]   S. Zhang, X. Qi, X. Ma, L. Lu, Y. Deng, Hydroxyl ionic liquids: The differentiating effect of  
21      hydroxyl on polarity due to ionic hydrogen bonds between hydroxyl and anions, *J. Phys.*  
22      *Chem. B.* 114 (2010) 3912–3920. doi:10.1021/jp911430t.
- 23   [16]   A.H. Jalili, A. Mehdizadeh, M. Shokouhi, H. Sakhaeina, V. Taghikhani, Solubility of CO<sub>2</sub> in  
24      1-(2-hydroxyethyl)-3-methylimidazolium ionic liquids with different anions, *J. Chem.*  
25      *Thermodyn.* 42 (2010) 787–791. doi:10.1016/j.jct.2010.02.002.
- 26   [17]   M. Fakhraee, B. Zandkarimi, H. Salari, M.R. Gholami, Hydroxyl-Functionalized 1-(2-  
27      Hydroxyethyl)-3-methyl Imidazolium Ionic Liquids Thermodynamic and Structural Properties  
28      using Molecular Dynamics Simulations and ab Initio Calculations, *J. Phys. Chem. B.* 118  
29      (2014) 14410–14428.
- 30   [18]   Y. Qu, C. Huang, Y. Song, J. Zhang, B. Chen, Efficient dehydration of glucose to 5-  
31      hydroxymethylfurfural catalyzed by the ionic liquid, 1-hydroxyethyl-3-methylimidazolium



- 1 tetrafluoroborate, *Bioresour. Technol.* 121 (2012) 462–466.  
2 doi:10.1016/j.biortech.2012.06.081.
- 3 [19] M. Shokouhi, M. Adibi, A.H. Jalili, M. Hosseini-jenab, A. Mehdizadeh, Solubility and Diffusion  
4 of H<sub>2</sub>S and CO<sub>2</sub> in the Ionic Liquid 1-(2-Hydroxyethyl)-3-methylimidazolium  
5 Tetrafluoroborate, *J. Chem. Eng. Data.* 55 (2010) 1663–1668.
- 6 [20] K. Kim, S. Park, S. Choi, H. Lee, Vapor Pressures of the 1-Butyl-3-methylimidazolium  
7 Bromide + Water , 1-Butyl-3-methylimidazolium Tetrafluoroborate + Water , and 1- ( 2-  
8 Hydroxyethyl ) -3-methylimidazolium Tetrafluoroborate + Water Systems, *J. Chem. Eng.*  
9 *Data.* 49 (2004) 1550–1553. doi:10.1021/je034210d.
- 10 [21] A. Cera-Manjarres, Experimental determination and modelling of thermophysical properties  
11 of ammonia/ionic liquid mixtures for absorption refrigeration systems, Universitat Rovira i  
12 Virgili, 2015.
- 13 [22] R. Rives, A. Mialdun, V. Yasnou, V. Shevtsova, A. Coronas, Experimental determination and  
14 predictive modelling of the mutual diffusion coefficients of water and ionic liquid 1-(2-  
15 hydroxyethyl)-3-methylimidazolium tetrafluoroborate, *J. Mol. Liq.* 296 (2019) 111931.  
16 doi:10.1016/j.molliq.2019.111931.
- 17 [23] M.M. Taib, T. Murugesan, Density, refractive index, and excess properties of 1-butyl-3-  
18 methylimidazolium tetrafluoroborate with water and monoethanolamine, *J. Chem. Eng.*  
19 *Data.* 57 (2012) 120–126. doi:10.1021/je2007204.
- 20 [24] G. Carissimi, M.G. Montalbán, F.G. Díaz Baños, G. Villora, Density, Refractive Index and  
21 Volumetric Properties of Water–Ionic Liquid Binary Systems with Imidazolium-Based  
22 Cations and Tetrafluoroborate, Triflate and Octylsulfate Anions, *J. Chem. Eng. Data.* 64  
23 (2019) 979–994. doi:10.1021/acs.jced.8b00854.
- 24 [25] I. Bahadur, T.M. Letcher, S. Singh, G.G. Redhi, P. Venkatesu, D. Ramjugernath, Excess  
25 molar volumes of binary mixtures (an ionic liquid + water): A review, *J. Chem. Thermodyn.*  
26 82 (2015) 34–46. doi:10.1016/j.jct.2014.10.003.
- 27 [26] M.G. Montalbán, C.L. Bolívar, F.G. Díaz Baños, G. Villora, Effect of Temperature, Anion,  
28 and Alkyl Chain Length on the Density and Refractive Index of 1-Alkyl-3-methylimidazolium-  
29 Based Ionic Liquids, *J. Chem. Eng. Data.* 60 (2015) 1986–1996. doi:10.1021/je501091q.
- 30 [27] M.A. Iglesias-Otero, J. Troncoso, E. Carballo, L. Romaní, Density and refractive index in  
31 mixtures of ionic liquids and organic solvents: Correlations and predictions, *J. Chem.*

- 1 Thermodyn. 40 (2008) 949–956. doi:10.1016/j.jct.2008.01.023.
- 2 [28] M. Yahya, M.Z. Saghir, Measurement of optical contrast factors in ternary hydrocarbon  
3 mixtures, *Phys. Chem. Liq.* 54 (2015) 74–97. doi:10.1080/00319104.2015.1084879.
- 4 [29] V. Shevtsova, V. Sechenyh, A. Nepomnyashchy, J.C. Legros, Analysis of the application of  
5 optical two-wavelength techniques to measurement of the Soret coefficients in ternary  
6 mixtures, *Philos. Mag.* 91 (2011) 3498–3518. doi:10.1080/14786435.2011.586376.
- 7 [30] M. Gebhardt, W. Köhler, A. Mialdun, V. Yasnou, V. Shevtsova, Diffusion, thermal diffusion,  
8 and Soret coefficients and optical contrast factors of the binary mixtures of dodecane,  
9 isobutylbenzene, and 1,2,3,4-tetrahydronaphthalene, *J. Chem. Phys.* 138 (2013) 114503.  
10 doi:10.1063/1.4795432.
- 11 [31] V. V. Sechenyh, J.C. Legros, V. Shevtsova, Optical properties of binary and ternary liquid  
12 mixtures containing tetralin, isobutylbenzene and dodecane, *J. Chem. Thermodyn.* 62  
13 (2013) 64–68. doi:10.1016/j.jct.2013.01.026.
- 14 [32] G.R. Chaudhary, S. Bansal, S.K. Mehta, A.S. Ahluwalia, Thermophysical and spectroscopic  
15 studies of pure 1-butyl-3- methylimidazolium tetrafluoroborate and its aqueous mixtures, *J.*  
16 *Solution Chem.* 43 (2014) 340–359. doi:10.1007/s10953-014-0137-8.
- 17 [33] R.R. Pinto, D. Santos, S. Mattedi, M. Aznar, Density, refractive index, apparent volumes and  
18 excess molar volumes of four protic ionic liquids + water at T=298.15 and 323.15 K, Brazilian  
19 *J. Chem. Eng.* 32 (2015) 671–682. doi:10.1590/0104-6632.20150323s00003444.
- 20 [34] D.G. Archer, J.A. Widegren, D.R. Kirklin, J.W. Magee, Enthalpy of solution of 1-Octyl-3-  
21 methylimidazolium tetrafluoroborate in water and in aqueous sodium fluoride, *J. Chem. Eng.*  
22 *Data.* 50 (2005) 1484–1491. doi:10.1021/je050136i.
- 23 [35] C. Villagrán, M. Deetlefs, W.R. Pitner, C. Hardacre, Quantification of Halide in Ionic Liquids  
24 Using Ion Chromatography, *Anal. Chem.* 76 (2004) 2118–2123. doi:10.1021/ac035157z.
- 25 [36] R.D. Chirico, M. Frenkel, J.W. Magee, V. Diky, C.D. Muzny, A.F. Kazakov, K. Kroenlein, I.  
26 Abdulagatov, G.R. Hardin, W.E. Acree, J.F. Brenneke, P.L. Brown, P.T. Cummings, T.W.  
27 De Loos, D.G. Friend, A.R.H. Goodwin, L.D. Hansen, W.M. Haynes, N. Koga, A. Mandelis,  
28 K.N. Marsh, P.M. Mathias, C. McCabe, J.P. O’Connell, A. Pádua, V. Rives, C. Schick, J.P.M.  
29 Trusler, S. Vyazovkin, R.D. Weir, J. Wu, Improvement of quality in publication of  
30 experimental thermophysical property data: Challenges, assessment tools, global  
31 implementation, and online support, *J. Chem. Eng. Data.* 58 (2013) 2699–2716.

- 1       doi:10.1021/je400569s.
- 2   [37] D. Chęcińska-Majak, K. Klimaszewski, M. Stańczyk, A. Bald, R.J. Sengwa, S. Choudhary,  
3       Static permittivity, density, speed of sound, and refractive index of 2-propoxyethanol  
4       mixtures with water in a wide temperature range, *J. Chem. Thermodyn.* 102 (2016) 164–  
5       177. doi:10.1016/j.jct.2016.07.002.
- 6   [38] F.A. Philip, D. Nath, K. Sibilla, A. Henni, Volumetric properties, viscosities and refractive  
7       indices of {3-diethylamino propylamine (DEAPA) + water} system from 293.15 K to 343.15 K,  
8       *J. Chem. Thermodyn.* 142 (2020) 105978. doi:10.1016/j.jct.2019.105978.
- 9   [39] L.C. Branco, J.N. Rosa, J.J. Moura Ramos, C.A.M. Afonso, Preparation and characterization  
10       of new room temperature ionic liquids, *Chem. - A Eur. J.* 8 (2002) 3671–3677.  
11       doi:10.1002/1521-3765(20020816)8:16<3671::AID-CHEM3671>3.0.CO;2-9.
- 12   [40] X. Hu, J. Yu, H. Liu, Liquid-Liquid Equilibria of the System 1-(2-Hydroxyethyl)-3-  
13       methylimidazolium Tetrafluoroborate + Water + 1-Butanol at 293.15 K, *J. Chem. Eng. Data.*  
14       51 (2006) 691–695.
- 15   [41] J. Restolho, A.P. Serro, J.L. Mata, B. Saramago, Viscosity and Surface Tension of 1-  
16       Ethanol-3-methylimidazolium Tetrafluoroborate and 1-Methyl-3-octylimidazolium  
17       Tetrafluoroborate over a Wide Temperature Range, *J. Chem. Eng. Data.* 54 (2009) 950–  
18       955.
- 19   [42] D. Song, J. Chen, Densities and viscosities for ionic liquids mixtures containing  
20       [eOHmim][BF<sub>4</sub>], [bmim][BF<sub>4</sub>] and [bpy][BF<sub>4</sub>], *J. Chem. Thermodyn.* 77 (2014) 137–143.  
21       doi:10.1016/j.jct.2014.05.016.
- 22   [43] E. Vercher, F.J. Llopis, V. González-Alfaro, P.J. Miguel, V. Orchillés, A. Martínez-Andreu,  
23       Volumetric properties, viscosities and refractive indices of binary liquid mixtures of  
24       tetrafluoroborate-based ionic liquids with methanol at several temperatures, *J. Chem.*  
25       *Thermodyn.* 90 (2015) 174–184. doi:10.1016/j.jct.2015.06.036.
- 26   [44] L.W. Tilton, J.K. Taylor, Refractive Index and dispersion of distilled water for visible radiation,  
27       at temperatures 0 to 60° C, *J. Res. Natl. Bur. Stand.* (1934). 20 (1938) 419.  
28       doi:10.6028/jres.020.024.
- 29   [45] R.N. O'Brien, Some Electrolyte Solution Refractive Indices at 5893 and 6328 Å, *J. Chem.*  
30       *Eng. Data.* 13 (1968) 2–5. doi:10.1021/je60036a001.
- 31   [46] E.M. Stanley, Refractive Index of Pure Water for Wavelength of 6328 Å at High Pressure

- 1 and Moderate Temperature, *J. Chem. Eng. Data.* 16 (1971) 454–457.  
2 doi:10.1021/je60051a029.
- 3 [47] G.M. Hale, M.R. Querry, Optical Constants of Water in the 200-nm to 200- $\mu$ m Wavelength  
4 Region, *Appl. Opt.* 12 (1973) 555–563. doi:10.1364/ao.12.000555.
- 5 [48] P. Brocos, Á. Piñeiro, R. Bravo, A. Amigo, Refractive indices, molar volumes and molar  
6 refractions of binary liquid mixtures: Concepts and correlations, *Phys. Chem. Chem. Phys.*  
7 5 (2003) 550–557. doi:10.1039/b208765k.
- 8 [49] T.S. Krishna, M.G. Sankar, A.K. Nain, B. Munibhadrayya, Temperature dependent study of  
9 thermophysical and optical properties of binary mixtures of imidazolium based ionic liquids,  
10 *Indian J. Chem. - Sect. A Inorganic, Phys. Theor. Anal. Chem.* 55A (2016) 664–675.
- 11 [50] M. Anouti, A. Vigeant, J. Jacquemin, C. Brigouleix, D. Lemordant, Volumetric properties,  
12 viscosity and refractive index of the protic ionic liquid, pyrrolidinium octanoate, in molecular  
13 solvents, *J. Chem. Thermodyn.* 42 (2010) 834–845. doi:10.1016/j.jct.2010.01.013.
- 14 [51] W. Heller, Remarks on refractive index mixture rules, *J. Phys. Chem.* 69 (1965) 1123–1129.  
15 doi:10.1021/j100888a006.
- 16